

Robust and Information-theoretically Safe Bias Classifier against Adversarial Attacks*

Lijia Yu and Xiao-Shan Gao

Academy of Mathematics and Systems Science, Chinese Academy of Sciences,
Beijing 100190, China

University of Chinese Academy of Sciences, Beijing 100049, China

Email: xgao@mmrc.iss.ac.cn

Abstract

In this paper, the bias classifier is introduced, that is, the bias part of a DNN with Relu as the activation function is used as a classifier. The work is motivated by the fact that the bias part is a piecewise constant function with zero gradient and hence cannot be directly attacked by gradient-based methods to generate adversaries such as FGSM. The existence of the bias classifier is proved an effective training method for the bias classifier is proposed. It is proved that by adding a proper random first-degree part to the bias classifier, an information-theoretically safe classifier against the original-model gradient-based attack is obtained in the sense that the attack generates a totally random direction for generating adversaries. This seems to be the first time that the concept of information-theoretically safe classifier is proposed. Several attack methods for the bias classifier are proposed and numerical experiments are used to show that the bias classifier is more robust than DNNs against these attacks in most cases.

Keywords. Robust DNN, adversarial samples, bias classifier, information-theoretically safe, gradient-based attack.

1 Introduction

The deep neural network (DNN) [18] has become the most powerful machine learning method, which has been successfully applied in computer vision, natural language processing, game playing, protein structure prediction, and many other fields.

One of the problems of DNN is the existence of adversaries [27], that is, it is possible to intentionally make little modifications to an input such that human can still recognize the input clearly, but the DNN outputs a wrong label or even any label given by the adversary. Existence of adversarial samples makes the DNN vulnerable in safety-critical applications. Although many effective methods to defend adversaries were proposed [1, 4, 37], it was shown that adversaries seem still inevitable for current DNNs [3, 23]. In this paper, we present a new approach by using the bias part as the classifier and show that the bias classifier is safe against adversaries in certain sense.

*This work is partially supported by NSFC grant No.11688101 and NKRDP grant No.2018YFA0306702.

1.1 Contributions

Let $\mathbb{I} = [0, 1] \subset \mathbb{R}$ and $\mathcal{F} : \mathbb{I}^n \rightarrow \mathbb{R}^m$ a classification DNN for m objects, using Relu as the activation function. For any $x \in \mathbb{I}^n$, there exist $W_x \in \mathbb{R}^{m \times n}$ and $B_x \in \mathbb{R}^m$ such that

$$\mathcal{F}(x) = W_x x + B_x$$

where $W_x x$ is called the *first-degree part* and B_x the *bias part* of \mathcal{F} . From the definition of the Relu function, the bias part

$$B_{\mathcal{F}} : \mathbb{I}^n \rightarrow \mathbb{R}^m$$

defined as $B_{\mathcal{F}}(x) = B_x$ is a piecewise constant function with a finite number of values.

The most popular and effective methods to generate adversaries, such as FGSM [11] or PGD [20], use $\frac{\nabla \mathcal{F}(x)}{\nabla x}$ to make the loss function bigger. An attack on DNNs only using the values of $\mathcal{F}(x)$ and $\frac{\nabla \mathcal{F}(x)}{\nabla x}$ is called a *gradient-based attack*. Since n is generally quite large, using $\frac{\nabla \mathcal{F}(x)}{\nabla x}$ to find adversaries in the high-dimensional space \mathbb{R}^n seems inevitable.

Motivated by the above observation, the bias classifier is introduced in this paper, that is, the bias part $B_{\mathcal{F}} : \mathbb{I}^n \rightarrow \mathbb{R}^m$ of \mathcal{F} is used to classify the m objects. Since $B_{\mathcal{F}}$ is a piecewise constant function, it has zero gradient and is safe against direct gradient-based attacks. The contributions of this paper are summarized below.

First, the existence of the bias classifier is proved. Precisely, it is proved that for any classification problem, there exists a DNN \mathcal{F} such that its bias part $B_{\mathcal{F}}$ gives the correct label for the classification problem with arbitrarily high probability.

Second, an effective training method for the bias classifier is proposed. It is observed that the adversarial training method introduced in [20] significantly increases the classification power of the bias part. Furthermore, using the adversarial training method to the loss function $L_{CE}(B_{\mathcal{F}}(x), y) + \gamma L_{CE}(\mathcal{F}(x), y)$ increases the classification power of the bias part and decreases the classification power of first-degree part of \mathcal{F} , and hence is used to train the bias classifier.

Third, an *information-theoretically safe* bias classifier is given. The notion of *information-theoretically safe*, also called perfectly safe, is borrowed from cryptography [9, p.476], which means that the ciphertext yields no information regarding the plaintext for cyphers which are perfectly random. Let $W_R \in \mathbb{R}^{m \times n}$ be a random matrix satisfying certain distributions, $\mathcal{F} : \mathbb{I}^n \rightarrow \mathbb{R}^m$ a trained bias classifier, and $\tilde{\mathcal{F}}(x) = \mathcal{F}(x) + W_R x$. Then, it is shown that $B_{\tilde{\mathcal{F}}}$ is information-theoretically safe against certain gradient-based attacks of $\tilde{\mathcal{F}}$, if the structure and parameters of \mathcal{F} are kept secret. A network \mathcal{F} is called *information-theoretically safe* against an attack \mathcal{A} , if when generating adversaries for an image x , the attack \mathcal{A} gives a random direction to generate adversaries, or equivalently, the adversary creation rate of \mathcal{F} under the attack \mathcal{A} is equal to the rate of certain random samples to be adversaries.

Fourth, several methods to attack the bias classifier are proposed. Experiments with MNIST and CIFAR-10 data sets show that the bias classifier is more robust than DNNs against these adversarial attacks in most cases.

1.2 Related work

There exist two main approaches to obtain more robust DNNs: using a better training method or a better structure for the DNN. Of course, the two approaches can be combined.

Many effective methods were proposed to train more robust DNNs to defend adversaries [1, 4, 37, 33]. The adversarial training method proposed by Madry et al [20] can reduce the adversaries significantly, where the value of the loss function of the worst adversary in a small neighborhood of the training sample is minimized. A similar approach is to generate adversaries and add them to the training set [11]. A fast adversarial training algorithm was proposed, which improves the training efficiency by reusing the backward pass calculations [24]. A less direct approach to resist adversaries is to make the DNN more stable by introducing the Lipschitz constant or $L_{p,\infty}$ regulations of each layer [5, 27, 35, 34]. Adding noises to the training data is an effective way to increase the robustness [10, Sec.7.5]. Knowledge distilling is also used to enhance robustness and defend adversarial examples [15].

In this paper, the adversarial training method [20] is used to a new loss function to train the bias classifier.

Many effective new structures for DNNs were proposed to defend adversaries [1, 4, 37, 33]. The ensembler adversarial training [28] was introduced for CNN models, which can apply to large datasets such as ImageNet. In [32], a denoising layer is added to each hidden layer to defend adversarial attack. In [16], differential privacy noise layers are added to defend adversaries. In [22], a low-rank DNN is shown to be more robust. In [36], a classification-autoencoder was proposed, which is robust against outliers and adversaries. In [6], it was observed that by taking average values of points in a small neighbourhood of an input can give a larger robust region for the input. In [12, 31], strategies to defend adversarial attacks by modifying the input were given.

In this paper, a new idea to obtain robust DNNs is given, that is, the bias part is used as the classifier to avoid gradient-based attacks. Another advantage of using the bias part as the classifier is that, an information-theoretically safe classifier can be constructed. The bias classifier does not deliberately hide the gradient like the method in [2], so the white box attack method for the gradient hiding method in [2] does not work for it.

The rest of this paper is organized as follows. In section 2, the existence of the bias classifier is proved and the training method is given. In section 3, several attack methods for the bias classifier are given. In section 4, the bias classifier is shown to be information-theoretically safe against the original-model gradient-based attack. In section 5, numerical experimental results are given to show that the bias classifier indeed improves robustness to resist adversaries. In section 6, conclusions are given

2 Classification using the bias part of DNN

In this section, we prove the existence of a DNN \mathcal{F} such that the bias part of \mathcal{F} can be used as a classifier. We also give the training algorithm for the new classifier.

2.1 The standard DNN

Denote $\mathbb{I} = [0, 1] \subset \mathbb{R}$ and $[n] = \{1, \dots, n\}$ for $n \in \mathbb{N}_{>0}$. In this paper, we assume that $\mathcal{F} : \mathbb{I}^n \rightarrow \mathbb{R}^m$ is a classification DNN for m objects, which has L hidden-layer, each hidden-layer has n nodes and uses Relu as activity functions, and the output layer does not have activity functions. We write \mathcal{F} as:

$$\begin{aligned} x_l &= \text{Relu}(W_l x_{l-1} + b_l) \in \mathbb{R}^{n_l}, W_l \in \mathbb{R}^{n_l \times n_{l-1}}, b_l \in \mathbb{R}^{n_l}, l \in [L]; \\ \mathcal{F}(x_0) &= x_{L+1} = W_{L+1} x_L + b_{L+1}, W_{L+1} \in \mathbb{R}^{m \times n}, b_{L+1} \in \mathbb{R}^m \end{aligned} \quad (1)$$

where $x_0 \in \mathbb{I}^n$, $n_0 = n$, $n_{L+1} = m$. Denote $\Theta_{\mathcal{F}} = \{W_l, b_l\}_{l=1}^{L+1}$ to be the parameter set of \mathcal{F} . Given a training set \mathcal{S} , the network \mathcal{F} can be trained as follows

$$\min_{\Theta} \sum_{(x,y) \in \mathcal{S}} L_{\text{CE}}(\mathcal{F}(x), y). \quad (2)$$

For any $x \in \mathbb{I}^n$, there exist $W_x \in \mathbb{R}^{m \times n}$ and $B_x \in \mathbb{R}^m$, such that $\mathcal{F}(x) = W_x x + B_x$. We define the *first-degree part* of \mathcal{F} to be $W_{\mathcal{F}} : \mathbb{I}^n \rightarrow \mathbb{R}^m$, that is $W_{\mathcal{F}}(x) = W_x x$; and the *bias part* of \mathcal{F} to be $B_{\mathcal{F}} : \mathbb{I}^n \rightarrow \mathbb{R}^m$, that is $B_{\mathcal{F}}(x) = B_x$. It is easy to see that

$$\mathcal{F}(x) = W_{\mathcal{F}}(x) + B_{\mathcal{F}}(x) = W_x x + B_x. \quad (3)$$

For a label $y \in [m]$ and $x \in \mathbb{I}^n$, denote $\mathcal{F}_y(x)$ to be the y -th coordinate of $\mathcal{F}(x)$.

A *linear region* of \mathcal{F} is a maximal connected open subset of the input space \mathbb{I}^n , on which \mathcal{F} is linear [11]. On each linear region A of \mathcal{F} , there exist $W_A \in \mathbb{R}^{m \times n}$ and $B_A \in \mathbb{R}^m$, such that $\mathcal{F}(x) = W_A x + B_A$ for $x \in A$. Due to the property of Relu function, it is clear that \mathcal{F} has a finite number of disjoint linear regions and \mathbb{I}^n is the union of the closures of these linear regions.

2.2 Existence of bias classifier

In this section, we will prove that the bias part $B_{\mathcal{F}}$ of \mathcal{F} can be used as a classifier. Let $\mathbb{O} \subset \mathbb{I}^n$ be the objects to be classified. For $x \in \mathbb{O}$ and $r \in \mathbb{R}_{>0}$, when r is small enough, all images in

$$\mathbb{B}(x, r) = \{x + \eta \mid \eta \in \mathbb{R}^n, \|\eta\| < r\}$$

can be considered to have the same label with x . Therefore, the object \mathbb{O} to be classified may be considered as bounded open sets in \mathbb{I}^n . This observation motivates the following existence theorem, whose proof will be given in this section. For $D \subset \mathbb{R}^n$, denote $V(D)$ to be the volume of D .

Theorem 2.1. *Let $\mathbb{O} = \bigcup_{i=1}^m O_i$ be the elements to be classified and $\mathbb{L} = \{l\}_{l=1}^m$ the label set, where $O_i \subset \mathbb{I}^n$ is an open set, $O_i \cap O_j = \emptyset$ if $i \neq j$, and x has label l for $x \in O_l$. Then for any $\epsilon > 0$, there exist a DNN \mathcal{F} and a $D \subset \mathbb{I}^n$ with $V(D) < \epsilon$, such that $B_{\mathcal{F}}(x)$ gives the correct label for $x \in O \setminus D$, that is, the l -th coordinate of $B_{\mathcal{F}}(x)$ has the largest value among all coordinates of $B_{\mathcal{F}}(x)$ for $x \in O_l \setminus D$.*

A network satisfying the conditions of Theorem 2.1 gives a *bias classifier*, which can be computed from \mathcal{F} as follows since $W_{\mathcal{F}}(x) = \frac{\nabla \mathcal{F}(x)}{\nabla x} \cdot x$, we have

$$B_{\mathcal{F}}(x) = \mathcal{F}(x) - W_{\mathcal{F}}(x) = \mathcal{F}(x) - \frac{\nabla \mathcal{F}(x)}{\nabla x} \cdot x. \quad (4)$$

We first prove several lemmas. In this section, the notations $\mathbb{O}, O_l, \mathbb{L}$ introduced in Theorem 2.1 will be used without mention. We will use another activation function $\Gamma : \mathbb{R} \rightarrow \mathbb{R}$

$$\Gamma(x) = \begin{cases} 0 & \text{if } x \leq 0 \\ 1 & \text{if } x > 0 \end{cases}.$$

Lemma 2.1 (Theorem 5 in [7]). *Let $l \in \mathbb{L}$ and $F_l : \mathbb{R} \rightarrow \mathbb{R}$ be a function such that $F_l(x) = 1$ if $x \in O_l$ and $F_l(x) = -1$ otherwise. Then for any $\epsilon > 0$, there exist $N \in \mathbb{N}_{>0}$, $W \in \mathbb{R}^{N \times n}$, $b \in \mathbb{R}^{N \times 1}$, $U \in \mathbb{R}^{1 \times N}$, and $D \in \mathbb{I}^n$ with $V(D) < \epsilon$, such that $|G(x) - F_l(x)| < \epsilon$ for $x \in \mathbb{O} \setminus D$, where $G(x) = U \cdot \Gamma(Wx + b)$.*

The following lemma shows that there exists a DNN with one hidden layer and using Γ as the activation function, which can be used as a classifier for \mathbb{O} .

Lemma 2.2. *For any $\epsilon > 0$, there exist $N \in \mathbb{N}_{>0}$, $W \in \mathbb{R}^{N \times n}$, $b \in \mathbb{R}^{N \times 1}$, $U \in \mathbb{R}^{1 \times N}$, and $D \in \mathbb{I}^n$ with $V(D) < \epsilon$, such that*

$$G(x) = U \cdot \Gamma(Wx + b) : \mathbb{I}^n \rightarrow \mathbb{R}^m$$

gives the correct label for $x \in \mathbb{O} \setminus D$, that is, the l -th coordinate of $G(x)$ has the biggest value for $x \in O_l$.

Proof. By Lemma 2.1, for $l \in \mathbb{L} = [m]$, there exist $N_a \in \mathbb{N}_{>0}$, $W_l \in \mathbb{R}^{(N_l, n)}$, $b_l \in \mathbb{R}^{(N_l, 1)}$, $U_l \in \mathbb{R}^{(1, N_l)}$, and $D_l \in \mathbb{I}^n$ with $m(D_l) < \epsilon/n$ such that

$$G_l(x) = U_l \cdot \Gamma(W_l x + b_l) \text{ and } |G_l(x) - F_l(x)| < \epsilon/n$$

for $x \in \mathbb{O} \setminus D$, where F_l is defined in lemma 2.1. Let $N = N_a m$, $W \in \mathbb{R}^{(N, n)}$, $b \in \mathbb{R}^{(N, 1)}$, where the l -th row of W is the l_2 -th row of W^{l_1} , the l -th row of b is the l_2 -th row of b^{l_1} , for $l = l_1 N_w + l_2$, $1 \leq l_2 \leq N_w$, and $l_1 \in [m]$.

Let $V \in \mathbb{R}^{(m, N)}$ be formed as follows: for $j \in [m]$, the j -th row of U_1 are zeros except the $j(N_w - 1) + 1$ -th to the $j(N_w - 1) + N_w$ -th rows, and the values of the $(j(N_w - 1) + k)$ -th place of the j -th row of U_1 equal to the values of the k -th place of U_l , where $k \in [N_a]$.

Now for $N \in \mathbb{N}_{>0}$, $W \in \mathbb{R}^{(N, n)}$, $b \in \mathbb{R}^{(N, 1)}$, $U \in \mathbb{R}^{(m, N)}$,

$$G(x) = U \cdot \Gamma(Wx + b)$$

satisfies $G(x)_l = G_l(x)$, where $G(x)_l$ is the l -th coordinate of $G(x)$. So there exist a set $D = \bigcup D_l \in \mathbb{I}^n$ with $m(D) < \epsilon$, such that $G(x)_y > 1 - \epsilon$ and $G(x)_l < -1 + \epsilon$ for $l \neq l_x$, where l_x is the label of x . Hence, $G(x)$ gives the correct label for $x \in \mathbb{O} \setminus D$. \square

Lemma 2.3. *The bias vector b in Lemma 2.2 can be chosen to consist of nonzero values.*

Proof. By Lemma 2.2, there exist N , W , b , U , and $D_1 \in \mathbb{I}^n$ with $V(D_1) < \epsilon/2$, such that

$$G(x) = U \Gamma(Wx + b)$$

gives the correct label for $x \in \mathbb{O} \setminus D_1$. Now assume $b_\gamma = b + I_0(b)\gamma$, where $I_0(x) = 1 - \text{sign}(|x|)$ and when I_0 is used as function of a matrix or a vector, it acts on each entry of this matrix or vector. We know that b_γ does not have zero parameters. Moreover, if $\Gamma(Wx + b) \neq \Gamma(Wx + b_\gamma)$, then there exists an $i \in [N]$ such that $W^i x + b^i > 0$ and $W^i x + b_\gamma^i < 0$ or $W^i x + b^i < 0$ and $W^i x + b_\gamma^i > 0$, where W^i is the i -th row of W , b^i and b_γ^i are respectively the i -th row of b and b_γ . Note that $\|W^i x + b_\gamma^i - W^i x + b^i\|_2 \leq \gamma$ when $x \in I_n$. If $W^i z + b^i > 0$ and $W^i z + b_\gamma^i < 0$ or $W^i z + b^i < 0$ and $W^i z + b_\gamma^i > 0$ for $z \in \mathbb{R}^n$, then we have $|W^i z + b^i| < \gamma$. Assume $Z_i = \{z \mid |W^i z + b^i| < \gamma\}$. We have $m(Z_I \cap I_0) < 2\gamma C_n$. The volume of the intersection of any hyperplane $C \in \mathbb{R}^n$ with \mathbb{I}_n must have an upper bound, which is denoted as C_n .

Let $Z = \{z \mid \Gamma(Wx + b) \neq \Gamma(Wx + b_\gamma)\}$. Then we have $m(Z \cap I_n) < 2\gamma N C_n$. Now let $\gamma = \frac{\epsilon}{4NC_n}$. Then there exists a $D = D_1 \cup (Z \cap I_n)$ such that $D_1 \in I_n$ and $m(D) < m(D_1) + 2\gamma N C_n < \epsilon$. Furthermore, for $x \in \mathbb{O} \setminus D$, we have $\Gamma(Wx + b) = \Gamma(Wx + b_\gamma)$. Then it is easy to know that, there exist N , W , b_γ , U , $D \in \mathbb{I}^n$ with $m(D) < \epsilon$ such that

$$G(x) = U \Gamma(Wx + b_\gamma)$$

gives the correct label for $x \in O \setminus D_1$, and b_γ do not have zero entries. The lemma is proved. \square

Lemma 2.4. Let $\mathcal{F}_1 : \mathbb{I}^n \rightarrow \mathbb{R}^m$ be a one-hidden-layer DNN with activation function $\Gamma(x)$, and any coordinate of its bias vector is nonzero. Then there exists a DNN \mathcal{F} , which has the same structure as \mathcal{F}_1 , except that the activation function of \mathcal{F} is Relu, such that $B_{\mathcal{F}}(x) = \mathcal{F}_1(x)$ for all $x \in \mathbb{I}^n$.

Proof. Assume $\mathcal{F}_1(x) = U\Gamma(Wx + b) + c$. Let $\mathcal{F}(x) = W^{\mathcal{F}_1}\text{Relu}(W^{\mathcal{F}}x + b^{\mathcal{F}}) + c$, where $W^{\mathcal{F}_1} = W^1\text{diag}(\frac{b_i}{|b_i|})$, $W^{\mathcal{F}} = \text{diag}(|b_i|^{-1})W$, and $b^{\mathcal{F}} = b/|b|$ (position-wise division). Then \mathcal{F} satisfies the condition of the lemma. \square

We now prove Theorem 2.1.

Proof of Theorem 2.1. Because of Lemma 2.2, there exist a $D \in \mathbb{I}^n$ with $m(D) < \epsilon$ and a network G with one-hidden-layer and with activation function $\Gamma(x)$, such that $G(x)$ gives the correct label for $x \in \mathbb{O} \setminus D$. By Lemma 2.3, all the parameters of G are no zero. Then by Lemma 2.4, we can obtain a network \mathcal{F} such that $B_{\mathcal{F}} = G(x)$, and the theorem is proved. \square

2.3 Training the bias classifier

In order to increase the robustness of the network, we will use the adversarial training introduced in [20], which is the best practical training method to defend adversaries. Let (x, y) be a data in the training set \mathcal{S} . Then the adversarial training uses the following loss function for a given small $\varepsilon \in \mathbb{R}_{>0}$

$$\min_{\Theta} \max_{\|\zeta\| < \varepsilon} \sum_{(x,y) \in \mathcal{S}} L_{\text{CE}}(\mathcal{F}(x + \zeta), y). \quad (5)$$

In order to increase the power of the bias part $B_{\mathcal{F}}$, we use the following loss function

$$\min_{\Theta} \max_{\|\zeta\| < \varepsilon} \sum_{(x,y) \in \mathcal{S}} [L_{\text{CE}}(B_{\mathcal{F}}(x + \zeta), y) + \gamma L_{\text{CE}}(\mathcal{F}(x + \zeta), y)] \quad (6)$$

where γ is a super parameter. The training procedure is given in Algorithm 1.

We first use numerical experiments to show that the adversarial training can increase the classification power of $B_{\mathcal{F}}$. The accuracies of \mathcal{F} , $W_{\mathcal{F}}$, $B_{\mathcal{F}}$ on the test set for three kinds of training methods are given in Table 1, respectively.

	$W_{\mathcal{F}}$	$B_{\mathcal{F}}$	\mathcal{F}
Normal training (2)	98.80%	15.62%	99.09%
Adversarial training (5)	90.61%	98.77%	99.19%
Adversarial training (6)	0.28%	99.09 %	99.43%

Table 1: Accuracies of network Lenet-5 for MNIST

Algorithm 1 HTrain-1

Require:

The set of training data: $\mathcal{S} = \{(x_i, y_i)\}$;
 The initial value of the parameter set Θ : Θ_0 ;
 The super parameter: M_s, M_b, M_n .

Ensure: The trained parameters Θ .

In each iteration:

 Input Θ_k

 Let $L(x, y, \Theta) = L_{CE}(B_{\mathcal{F}\Theta}(x), y)$.

 Let $L_1(x, y, \Theta) = L_{CE}(\mathcal{F}\Theta(x), y)$.

 For $(x, y) \in \mathcal{S}$, do

 $i=0, x_0 = x$

 While $i < M_s$:

$$x_{i+1} = x_i - M_b \frac{\partial L(x_i, y, \Theta_k)}{\partial x_i}$$

$$i = i + 1$$

$$x = x_{i+1}$$

$$\text{Let } L(\Theta_k) = \frac{1}{|\mathcal{S}|} \sum_{x, y \in \mathcal{S}} L(x, y, \Theta_k).$$

$$\text{Let } L_1(\Theta_k) = \frac{1}{|\mathcal{S}|} \sum_{x, y \in \mathcal{S}} L_1(x, y, \Theta_k).$$

$$\text{Let } \nabla L = \frac{\partial(L(\Theta_k) + M_n L_1(\Theta_k))}{\partial \Theta_k}.$$

 Output $\Theta_{k+1} = \Theta_k + \gamma_k \nabla L$; γ_k is the stepsize at iteration k.

3 Attack methods for the bias classifier

In this section, several possible methods to attack the bias classifier are given.

3.1 Safety against gradient-based attack

The most popular methods to generate adversaries, such as FGSM [11] or PGD [20], use $\frac{\nabla \mathcal{F}(x)}{\nabla x}$ to make the loss function bigger. More precisely, adversaries are generated as follows

$$x \rightarrow x + \varepsilon \text{sign}\left(\frac{\nabla \text{Loss}_{\mathcal{F}}(x)}{\nabla x}\right) \quad (7)$$

for a small parameter $\lambda \in \mathbb{R}_{>0}$. It is easy to see that, $\frac{\nabla \text{Loss}_{\mathcal{F}}(x)}{\nabla x}$ can be obtained from $\frac{\nabla \mathcal{F}(x)}{\nabla x}$ for most loss functions such as L_{CE} . So, in the above attack, only the values of $\mathcal{F}(x)$ and $\frac{\nabla \mathcal{F}(x)}{\nabla x}$ are needed and the detailed structure of \mathcal{F} are not needed. Inspired by this, between the black-box or white-box DNN models, we consider a model in between. A DNN model is called a *gradient-based model*, if for $x \in \mathbb{I}^n$, the values of $\mathcal{F}(x)$ and $\frac{\nabla \mathcal{F}(x)}{\nabla x}$ are known, but the detailed structure of \mathcal{F} is not known. Correspondingly, an attack only uses the values of $\mathcal{F}(x)$ and $\frac{\nabla \mathcal{F}(x)}{\nabla x}$ is called *gradient-based attack*.

Since the derivative of $B_{\mathcal{F}}$ is always zero, a gradient-based attack against $B_{\mathcal{F}}$ becomes a black-box attack, and in this sense we say that the bias classifier is safe against gradient-based attack.

In the gradient-based model, we do not know the structure of \mathcal{F} , but we can calculate $B_{\mathcal{F}}(x)$ from $\frac{\nabla \mathcal{F}(x)}{\nabla x}$ are $\frac{\nabla \text{Loss}_{\mathcal{F}}(x)}{\nabla x}$ using (4).

3.2 Original-model attack

An obvious attack for the bias classifier is to create adversaries of $B_{\mathcal{F}}$ using the gradients of \mathcal{F} , which is called *original-model attack*. The algorithm is below, where $\widehat{B}_{\mathcal{F}}(x)$ is the label of $B_{\mathcal{F}}(x)$.

Algorithm 2 HAttack-1.1w

Require:

The value of the parameter Θ of \mathcal{F} ;
 The super parameters: $\epsilon \in \mathbb{R}$, $n \in \mathbb{N}$;
 A samples x_0 and its label y .

Ensure: An adversarial sample x_a .

```

 $x = x_0$ 
For  $i = 1, \dots, n$ :
    If  $\widehat{B}_{\mathcal{F}}(x) \neq y$ :
        Break.
     $x = x + \epsilon \text{sign}(\frac{\nabla \mathbb{L}_{CE}(\mathcal{F}(x), y)}{\nabla x})$ 
If  $\widehat{B}_{\mathcal{F}}(x) \neq y$ ,  $x_a = x$  output:  $x_a$ 
Output: No adversary for  $x_0$ 
```

3.3 Correlation attack on the bias classifier

From numerical experiments, we have the following observations. For a network $\mathcal{F} : \mathbb{I}^n \rightarrow \mathbb{R}^m$ trained with (6) and a small vector $\epsilon \in \mathbb{R}^n$, the following facts happen with high probability: $W_{\mathcal{F}}(x)[l] \geq W_{\mathcal{F}}(x')[l]$ if and only if $B_{\mathcal{F}}(x)[l] \leq B_{\mathcal{F}}(x')[l]$, where $l \in \mathbb{L}$ and $x' = x + \epsilon$. In other words, $W_{\mathcal{F}}$ and $B_{\mathcal{F}}$ are co-related and we thus can attack the $B_{\mathcal{F}}[l]$ by increasing $W_{\mathcal{F}}[l]$, which is called the *correlation attack*.

In the correlation attack, we create adversaries by making $W_{\mathcal{F}}(x)[y] - W_{\mathcal{F}}(x)[i]$ bigger, where y is the label of x , $i \in [m]$ and $i \neq y$. The attack procedure is given below.

Algorithm 3 HAttack-1.1

Require:

The value of the parameters Θ of \mathcal{F} ;
 The super parameters: $\epsilon \in \mathbb{R}$, $N \in \mathbb{N}$;
 A samples x_0 and its label y .

Ensure: An adversarial sample x_a .

```

For  $i \in \mathbb{L}$  and  $i \neq y$ :
     $x = x_0, j=0$ 
    While  $j < N$ :
         $W_{x,y} = \frac{\nabla \mathcal{F}_y(x)}{\nabla x}$ ,  $W_{x,i} = \frac{\nabla \mathcal{F}_i(x)}{\nabla x}$ ,  $W_{di} = W_{x,y} - W_{x,i}$ 
         $x = x + \epsilon W_{di}$ 
        if  $\widehat{B}_{\mathcal{F}}(x) \neq y$ 
            break
        else:
             $j=j+1$ 
            if  $j = N$ , break
        If  $\widehat{B}_{\mathcal{F}}(x) \neq y$ ,  $x_a = x$  output:  $x_a$ 
    Output: No adversary for  $x_0$ 
```

4 Information-theoretically safety against original-model gradient-based attack

By the original-model gradient-based attack, we mean using the gradient of \mathcal{F} to generate adversaries for $B_{\mathcal{F}}$. In this section, we show that it is possible to make the bias classifier safe against this kind of attack. The idea is to make $\frac{\nabla \mathcal{F}(x)}{\nabla x}$ random and $B_{\mathcal{F}}$ still gives the correct classification.

4.1 Safety of direct attack

We first train a DNN $\mathcal{F} : \mathbb{I}^n \rightarrow \mathbb{R}^m$ with the method in Section 2.3. Let $W_R \in \mathbb{R}^{m \times n}$ and $\mathcal{F}_R(x) = W_R x : \mathbb{R}^n \rightarrow \mathbb{R}^m$ be a random linear map and

$$\tilde{\mathcal{F}}(x) = \mathcal{F}(x) + \mathcal{F}_R(x) = \mathcal{F}(x) + W_R x. \quad (8)$$

Then, it is easy to see that $B_{\tilde{\mathcal{F}}} = B_{\mathcal{F}}$.

Let $\mathcal{U}(a, b)$ be the uniform distribution in $[a, b] \subset \mathbb{R}$. For $\lambda \in \mathbb{R}_{>0}$, denote $\mathcal{M}_{m,n}(\lambda)$ to be the random matrices such that the elements of its i -row are in $\mathcal{U}(-2i\lambda, -(2i-1)\lambda) \cup \mathcal{U}((2i-1)\lambda, 2i\lambda)$. It is easy to see that for $W_R \sim \mathcal{M}_{m,n}(\lambda)$, we have $\|W_{R,i} - W_{R,j}\|_{\infty} > \lambda$ for $i \neq j$, where $W_{R,i}$ is the i -th row of W_R .

For $\rho \in \mathbb{R}_{>0}$ consider the following gradient-based *direct attack* [39] for the network \mathcal{F} :

$$\mathcal{A}_1(x, \mathcal{F}, \rho) = x + \rho \operatorname{sign}\left(\frac{\nabla \mathcal{F}_{\bar{y}}(x)}{\nabla x} - \frac{\nabla \mathcal{F}_y(x)}{\nabla x}\right) \quad (9)$$

where y is the label of x and $\bar{y} = \arg \max_{i \neq y} \{\tilde{\mathcal{F}}_i(x)\}$.

Theorem 4.1. *Let $|\frac{\nabla \mathcal{F}(x)}{\nabla x}|_{\infty} < \lambda/2$ and $W_R \in \mathcal{M}_{m,n}(\lambda)$. If the structure and parameters of \mathcal{F} are kept secret, then $B_{\tilde{\mathcal{F}}}$ is information-theoretically safe against the attack $\mathcal{A}_1(x, \tilde{\mathcal{F}}, \rho)$ in the sense that attacking $B_{\tilde{\mathcal{F}}}$ using $\mathcal{A}_1(x, \tilde{\mathcal{F}}, \rho)$ gives a random direction $(\mathcal{A}_1(x, \mathcal{F}, \rho) - x)/\rho$ for generating adversaries.*

Proof. From (8), $\frac{\nabla \tilde{\mathcal{F}}(x)}{\nabla x} = \frac{\nabla \mathcal{F}(x)}{\nabla x} + \frac{\nabla \mathcal{F}_R(x)}{\nabla x} = W_x + W_R$. Let $W_{x,i}$ and $W_{R,i}$ to be the i -rows of W_x and W_R , respectively. If $W_R \sim \mathcal{M}_{m,n}(\lambda)$, then $\|W_{R,i} - W_{R,j}\|_{\infty} > \lambda$ for $i \neq j$. Since $|\frac{\nabla \mathcal{F}(x)}{\nabla x}|_{\infty} = |W_x|_{\infty} < \lambda/2$, we have $\|W_{x,i} - W_{x,j}\|_{\infty} < \lambda$ for $i \neq j$. Then from (9),

$$\begin{aligned} \mathcal{A}_1(x, \tilde{\mathcal{F}}, \rho) &= x + \rho \operatorname{sign}\left(\frac{\nabla \tilde{\mathcal{F}}_{\bar{y}}(x)}{\nabla x} - \frac{\nabla \tilde{\mathcal{F}}_y(x)}{\nabla x}\right) \\ &= x + \rho \operatorname{sign}(W_{x,\bar{y}} - W_{x,y} + W_{R,\bar{y}} - W_{R,y}) \\ &= x + \rho \operatorname{sign}(W_{R,\bar{y}} - W_{R,y}). \end{aligned} \quad (10)$$

Then $(\mathcal{A}_1(x, \mathcal{F}, \rho) - x)/\rho = W_{R,\bar{y}} - W_{R,y}$ is a random vector. \square

The notion of *information-theoretically safe*, also called perfectly safe, is borrowed from cryptography [9, p.476], which means that the ciphertext yields no information regarding the plaintext if the cyphers are perfectly random.

In the rest of this section, we give the exact adversary creation rate of $B_{\tilde{\mathcal{F}}}$ under attack \mathcal{A}_1 . We first introduce some notations. Let $\mathcal{A}(x, \mathcal{F}) : \mathbb{R}^n \rightarrow \mathbb{R}^n$ be an attack which tries to create an adversary $\mathcal{A}(x, \mathcal{F})$ for \mathcal{F} . Assume that W_R satisfies a given distribution $\mathcal{M}_{m,n}$ of random matrices

in $\mathbb{R}^{m,n}$. The safety of the original-model gradient-based attack to $B_{\tilde{\mathcal{F}}}$ under attack \mathcal{A} can be measured by the following adversary creation rate

$$\mathcal{C}(\mathcal{F}, \mathcal{A}, \mathcal{M}_{m,n}) = \mathbb{E}_{W_R \sim \mathcal{M}_{m,n}} [\mathbb{E}_{x \sim \mathcal{D}_0} [\mathbf{I}(\hat{B}_{\mathcal{F}}(\mathcal{A}(x, \tilde{\mathcal{F}})) \neq \hat{B}_{\mathcal{F}}(x))]] \quad (11)$$

where $\hat{B}_{\mathcal{F}}$ is the label of the classification and \mathcal{D}_0 is the distribution of the objects to be classified.

Corollary 4.1. *Under the same conditions in Theorem 4.1, we have*

$$\mathcal{C}(\mathcal{F}, \mathcal{A}_1, \mathcal{M}_{m,n}) = 1/2^n E_{x \sim \mathcal{D}_0} \sum_{V \in \{-1,1\}^n} [\mathbf{I}(\hat{B}_{\mathcal{F}}(x + \rho V) \neq \hat{B}_{\mathcal{F}}(x))]. \quad (12)$$

Proof. From (10), since $W_{R,\bar{y}} - W_{R,y}$ is a random vector whose entries having values in two intervals of the form $[-b_2, -b_1]$ and $[b_1, b_2]$ for $b_1, b_2 \in \mathbb{R}_{>0}$, we have

$$\begin{aligned} \mathcal{C}(\mathcal{F}, \rho) &= E_{x \sim \mathcal{D}_0} E_{W_R \sim \mathcal{M}_{m,n}(\lambda)} [\mathbf{I}(\hat{B}_{\mathcal{F}}(\mathcal{A}_1(x, \tilde{\mathcal{F}}, r)) \neq \hat{B}_{\mathcal{F}}(x))] \\ &= E_{x \sim \mathcal{D}_0} E_{W_R \sim \mathcal{M}_{m,n}(\lambda)} [\mathbf{I}(\hat{B}_{\mathcal{F}}(x + \rho \operatorname{sign}(W_{R,\bar{y}} - W_{R,y})) \neq \hat{B}_{\mathcal{F}}(x))] \\ &= 1/2^n E_{x \sim \mathcal{D}_0} \sum_{V \in \{-1,1\}^n} [\mathbf{I}(\hat{B}_{\mathcal{F}}(x + \rho V) \neq \hat{B}_{\mathcal{F}}(x))]. \end{aligned}$$

□

Note that $\mathcal{C}(\mathcal{F}, \mathcal{A}_1, \mathcal{M}_{m,n})$ depends only on \mathcal{F} and ρ , so denote

$$\mathcal{C}(\mathcal{F}, \rho) = 1/2^n E_{x \sim \mathcal{D}_0} \sum_{V \in \{-1,1\}^n} [\mathbf{I}(\hat{B}_{\mathcal{F}}(x + \rho V) \neq \hat{B}_{\mathcal{F}}(x))].$$

$\mathcal{C}(\mathcal{F}, \rho)$ can be used as a measure of the robustness of the bias classifier, which is the adversary rate of certain random samples. As shown in section 5.3.1, $\mathcal{C}(\mathcal{F}, \rho)$ is small for most networks when ρ is small.

From Corollary 4.1, we give another more precise meaning for the information-theoretically safety: a network \mathcal{F} is information-theoretically safe under certain attack \mathcal{A} if the adversary creation rate of \mathcal{F} under attack \mathcal{A} is equal to the rate of random samples to be adversaries.

4.2 Safety of FGSM attack

In this section, we show that the result in section 4.1 also holds for the FGSM attack if $m = 2$. Here is the FGSM attack:

$$\mathcal{A}_2(x, \mathcal{F}, \rho) = x + \rho \operatorname{sign}(\frac{\nabla L(\mathcal{F}(x), y)}{\nabla x}). \quad (13)$$

Theorem 4.2. *If $|\frac{\nabla \mathcal{F}(x)}{\nabla x}|_{\infty} < \lambda/2$ and $W_R \sim \mathcal{M}_{m,n}(\lambda)$, then $\mathcal{C}(\tilde{\mathcal{F}}, \mathcal{A}_2, \mathcal{M}_{m,n}(\lambda)) \leq \mathcal{C}(\tilde{\mathcal{F}}, \rho)$.*

Proof. Let $y \in \{0, 1\}$ be the label of x . Use the notations introduced in the proof of Theorem 4.1. Since the loss function is L_{CE} , we have

$$\begin{aligned} \frac{\nabla L(\tilde{\mathcal{F}}(x), y)}{\nabla x} &= \frac{1}{\sum_{i=1}^m e^{\tilde{\mathcal{F}}_i(x)}} (\sum_{i=1}^m e^{\tilde{\mathcal{F}}_i} (W_{x,i} - W_{x,y} + W_{R,i} - W_{R,y})) \\ &= \frac{e^{\tilde{\mathcal{F}}_{1-y}(x)}}{\sum_{i=1}^m e^{\tilde{\mathcal{F}}_i(x)}} ((W_{x,1-y} - W_{x,y} + W_{R,1-y} - W_{R,y}). \end{aligned}$$

The last equality comes from $m = 2$. Since $\|W_{x,i} - W_{x,j}\|_\infty < \lambda$ and $\|W_{R,i} - W_{R,j}\|_\infty > \lambda$ for $i \neq j$, we have

$$\text{sign}\left(\frac{\nabla L(\tilde{\mathcal{F}}(x), y)}{\nabla x}\right) = \text{sign}(W_{R,1-y} - W_{R,y}).$$

Then

$$\begin{aligned} \mathcal{C}(\mathcal{F}, \rho) &= E_{x \sim \mathcal{D}_0} E_{W_R \sim \mathcal{M}_{m,n}(\lambda)} [\mathbf{I}(\hat{B}_{\mathcal{F}}(\mathcal{A}_2(x, \tilde{\mathcal{F}}, r)) \neq \hat{B}_{\mathcal{F}}(x))] \\ &= E_{x \sim \mathcal{D}_0} E_{W_R \sim \mathcal{M}_{m,n}(\lambda)} [\mathbf{I}(\hat{B}_{\mathcal{F}}(x + \rho \text{sign}(W_{R,1-y} - W_{R,y})) \neq \hat{B}_{\mathcal{F}}(x))] \\ &= 1/2^n E_{x \sim \mathcal{D}_0} \sum_{V \in \{-1,1\}^n} [\mathbf{I}(\hat{B}_{\mathcal{F}}(x + \rho V) \neq \hat{B}_{\mathcal{F}}(x))] \\ &= \mathcal{C}(\mathcal{F}, \rho). \end{aligned}$$

The theorem is proved. \square

4.3 Safety of direct attack under simpler distribution

Let $\mathcal{U}_{m,n}(\lambda)$ be the random matrices whose entries are in $\mathcal{U}(-\lambda, \lambda)$. In this section, we show that the result in section 4.1 is true for $W_R \in \mathcal{U}_{m,n}(\lambda)$. We consider the multi-step direct attack \mathcal{A}_3 :

$$\begin{aligned} x^{(0)} &= x \\ x^{(i)} &= x^{(i-1)} + \frac{\rho}{k} \text{sign}\left(\frac{\nabla \mathcal{F}_{\bar{y}}(x^{(i-1)})}{\nabla x^{(i-1)}} - \frac{\nabla \mathcal{F}_y(x^{(i-1)})}{\nabla x^{(i-1)}}\right), i \in [k] \\ \mathcal{A}_3(x, \mathcal{F}, \rho) &= x^{(k)} \end{aligned} \tag{14}$$

where y is the label of x , $k \in \mathbb{N}_{>0}$ is a constant, and $\bar{y} = \arg \max_{i \neq y} \{\mathcal{F}_i(x)\}$.

Theorem 4.3. *If $|\frac{\nabla \mathcal{F}(x)}{\nabla x}|_\infty < \mu/2$ and $W_R \sim \mathcal{U}_{m,n}(\lambda)$, then $\mathcal{C}(\tilde{\mathcal{F}}, \mathcal{A}_3, \mathcal{U}_{m,n}(\lambda)) \leq \mathcal{C}(\mathcal{F}, \rho) + \mu a/\lambda$. If $\lambda > n\mu/\epsilon$, then $\mathcal{C}(\tilde{\mathcal{F}}, \mathcal{A}_3, \mathcal{U}_{m,n}(\lambda)) \leq \mathcal{C}(\mathcal{F}, \rho) + \epsilon$ for any $\epsilon \in \mathbb{R}_{>0}$, and in particular, if $\lambda > na/(\epsilon \mathcal{C}(\mathcal{F}, \rho))$, then $\mathcal{C}(\tilde{\mathcal{F}}, \mathcal{A}_3, \mathcal{U}_{m,n}(\lambda)) \leq (1 + \epsilon) \mathcal{C}(\mathcal{F}, \rho)$.*

The theorem implies that $\tilde{\mathcal{F}}$ is close to information-theoretically safe. We first prove a lemma.

Lemma 4.1. *Let $x_1, x_2 \sim U(-\lambda, \lambda)$ and $z = x_1 - x_2$. Then for $a \in [0, 2\lambda]$, we have $P(z < a) = P(z > -a) = T(\lambda, a) = 1 - \frac{(2\lambda-a)^2}{8\lambda^2}$.*

Proof. Let $f(z)$ be the density function of z . Then $f(z) = 0$, if $z \geq 2\lambda$ or $z \leq -2\lambda$; $f(z) = \frac{2\lambda+x}{4\lambda^2}$, if $0 \geq z \geq -2\lambda$; $f(z) = \frac{2\lambda-x}{4\lambda^2}$, if $0 \leq z \leq 2\lambda$. Hence, $P(z < a) = P(z > -a) = 1 - \frac{(2\lambda-a)^2}{8\lambda^2}$. \square

Note that $T(\lambda, a)$ increases with a and $T(\lambda, a) \in [0.5, 1]$.

We give the proof of Theorem 4.2.

Proof. Similar to (10), we have

$$\begin{aligned} \mathcal{A}_3(x, \tilde{\mathcal{F}}, \rho) &= x + \frac{\rho}{k} \sum_{i=1}^k \text{sign}(W_{x^{(i-1)}, \bar{y}} - W_{x^{(i-1)}, y} + W_{R, \bar{y}} - W_{R, y}) \\ &= x + \rho \sum_{i=1}^k \text{sign}(W_{R, \bar{y}} - W_{R, y}) \text{ if } \|W_{R, \bar{y}} - W_{R, y}\|_\infty > \mu. \end{aligned}$$

So by Lemma 4.1,

$$\begin{aligned} \mathcal{C}(\tilde{\mathcal{F}}, \mathcal{A}_3, \mathcal{U}_{m,n}(\lambda)) &= E_{x \sim \mathcal{D}_0} E_{W_R \sim \mathcal{U}_{m,n}(\lambda)} [\mathbf{I}(\hat{B}_{\mathcal{F}}(\mathcal{A}_2(x, \tilde{\mathcal{F}}, \rho)) \neq \hat{B}_{\mathcal{F}}(x))] \\ &\leq E_{x \sim \mathcal{D}_0} E_{W_R \sim \mathcal{U}_{m,n}(\lambda)} [P(\|W_{R, \bar{y}} - W_{R, y}\|_\infty \leq \mu) + P(\|W_{R, \bar{y}} - W_{R, y}\|_\infty > \mu) [\mathbf{I}(\hat{B}_{\mathcal{F}}(\mathcal{A}_2(x, \tilde{\mathcal{F}})) \neq \hat{B}_{\mathcal{F}}(x))] \\ &\leq (1 - 2^n(1 - T(\lambda, \mu))^n) + 2^n(1 - T(\lambda, \mu))^n E_{x \sim \mathcal{D}_0} \sum_{V \in \{-1,1\}^n} [\mathbf{I}(\hat{B}_{\mathcal{F}}(x + \rho(W_{R, \bar{y}} - W_{R, y})) \neq \hat{B}_{\mathcal{F}}(x))] \\ &\leq (1 - 2^n(1 - T(\lambda, \mu))^n) + 2^n(1 - T(\lambda, \mu))^n \mathcal{C}(\rho) \\ &= 1 - (1 - \mathcal{C}(\rho)) 2^n(1 - T(\lambda, \mu))^n \end{aligned}$$

where $T(\lambda, \mu) = 1 - \frac{(2\lambda - \mu)^2}{8\lambda^2}$. We have $2^n(1 - T(\lambda, \mu))^n = (2 - 2 + \frac{4\lambda^2 + \mu^2 - 4\lambda\mu}{4\lambda^2})^n = (1 - \frac{4\lambda\mu - \mu^2}{4\lambda^2})^n \geq 1 - n\frac{4\lambda\mu - \mu^2}{4\lambda^2} \geq 1 - n\mu/\lambda$. So,

$$\begin{aligned} \mathcal{C}_{\mathcal{A}_2}(\tilde{\mathcal{F}}) &\leq 1 - (1 - \mathcal{C}(\rho))2^n(1 - T(\lambda, \mu))^n \\ &\leq 1 - (1 - \mathcal{C}(\rho))(1 - n\mu/\lambda) \\ &\leq \mathcal{C}(\rho) + n\mu/\lambda. \end{aligned}$$

The theorem is proved. \square

4.4 Safety of FGSM under simpler distribution

In this section, show that the result in section 4.2 is true for the simpler distribution $\mathcal{U}_{m,n}(\lambda)$. Let \mathcal{A}_2 be the attack in (13). Then we have

Theorem 4.4. *If $|\frac{\nabla \mathcal{F}(x)}{\nabla x}|_\infty < \mu/2$, $W_R \sim \mathcal{U}_{m,n}(\lambda)$, and $m = 2$, then $\mathcal{C}(\tilde{\mathcal{F}}, \mathcal{A}_2, \mathcal{U}_{m,n}(\lambda)) \leq e^{n\mu/\lambda} \mathcal{C}(\mathcal{F}, \rho)$. Furthermore if $\lambda > n\mu/\ln(1 + \epsilon)$, then $\mathcal{C}(\tilde{\mathcal{F}}, \mathcal{A}_2, \mathcal{U}_{m,n}(\lambda)) \leq (1 + \epsilon) \mathcal{C}(\mathcal{F}, \rho)$.*

Proof. Let $y \in \{0, 1\}$ be the label of x . From the proof of Theorem 4.2, we have

$$\begin{aligned} \frac{\nabla L(\mathcal{F}(x), y)}{\nabla x} &= \frac{e^{\mathcal{F}_1-y(x)}}{\sum_{i=1}^m e^{\mathcal{F}_i(x)}} (W_{x,1-y} - W_{x,y}), \\ \frac{\nabla L(\tilde{\mathcal{F}}(x), y)}{\nabla x} &= \frac{e^{\tilde{\mathcal{F}}_1-y(x)}}{\sum_{i=1}^m e^{\tilde{\mathcal{F}}_i(x)}} ((W_{x,1-y} - W_{x,y} + W_{R,1-y} - W_{R,y})). \end{aligned}$$

Denote $a(x) = W_{x,1-y} - W_{x,y}$ and $b(y) = W_{R,1-y} - W_{R,y}$. Use $\alpha(U, V)$ to denote the angle between two vector U and V . We have

$$\alpha(\text{sign}(\frac{\nabla L(\mathcal{F}(x), y)}{\nabla x}), \text{sign}(\frac{\nabla L(\tilde{\mathcal{F}}(x), y)}{\nabla x})) = \alpha(\text{sign}(a(x)), \text{sign}(a(x) + b(y))).$$

For $i \in [n]$, $\text{sign}(a_i(x)) = \text{sign}(a_i(x) + b_i(y))$ if and only if $(b_i(y) \leq -a_i(x) \text{ and } a_i(x) \leq 0)$ or $(b_i(y) \geq -a_i(x) \text{ and } a_i(x) \geq 0)$, where $b_i(y), a_i(x)$ are respectively the i -th coordinate of $b(y), a(x)$. Since $W_R \sim \mathcal{U}_{m,n}(\lambda)$, $b_i(y) = W_{R,1-y} - W_{R,y}$ is the difference of two uniform distribution in $[-\lambda, \lambda]$. By Lemma 4.1, we have $a_i(x) > 0$ implies $P(b_i(y) \geq -a_i(x)) = T(\lambda, |a_i(x)|) < T(\lambda, \mu)$, and $a_i(x) < 0$ implies $P(b_i(y) \leq -a_i(x)) = T(\lambda, |a_i(x)|) < T(\lambda, \mu)$. Hence, no matter what is the value of $a(x)$, we always have $P(\text{sign}(a(x)) = \text{sign}(a(x) + b(y))) < T(\lambda, \mu)^n$.

Moreover, for $i \in [n]$, if $\text{sign}(a_i(x)) \neq \text{sign}(a_i(x) + b_i(y))$, we have $(b_i(y) > 0 \text{ when } a_i(x) < 0) \text{ or } (b_i(y) < 0 \text{ when } a_i(x) > 0)$. So, $P(\text{sign}(a_i(x)) \neq \text{sign}(a_i(x) + b_i(y))) < 1/2 < T(\lambda, \mu)$.

Since $\{b_i(y)\}_{i \in [n]}$ is iid, by Lemma 4.1, for any $V \in \{-1, 1\}^n$ we have

$$\begin{aligned} P_{W_R \sim \mathcal{U}_{m,n}(\lambda)}(\text{sign}(\frac{\nabla L(\tilde{\mathcal{F}}(x), y)}{\nabla x}) = V) &= P_{W_R \sim \mathcal{U}_{m,n}(\lambda)}(\text{sign}(a(x) + b(y)) = V) \\ &= \prod_{i=1}^n P_{W_R \sim \mathcal{U}_{m,n}(\lambda)}(\text{sign}(a_i(x) + b_i(y)) = V_i) \\ &= \prod_{i=1}^n (\mathbf{I}(\text{sign}(a_i(x)) = V_i) P_{W_R \sim \mathcal{U}_{m,n}(\lambda)}(\text{sign}(a_i(x)) = \text{sign}(a_i(x) + b_i(y))) \\ &\quad + \mathbf{I}(\text{sign}(a_i(x)) \neq V_i) P_{W_R \sim \mathcal{U}_{m,n}(\lambda)}(\text{sign}(a_i(x)) \neq \text{sign}(a_i(x) + b_i(y)))) \\ &\leq \prod_{i=1}^n (\mathbf{I}(\text{sign}(a_i(x)) = V_i) T(\lambda, \mu) + \mathbf{I}(\text{sign}(a_i(x)) \neq V_i) T(\lambda, \mu)) \\ &= T(\lambda, \mu)^n. \end{aligned}$$

For $V \in \{-1, 1\}^n$, denote $Q(x, V, \rho) = \mathbf{I}(\widehat{B}_{\mathcal{F}}(x + \rho V) \neq \widehat{B}_{\mathcal{F}}(x))$. We have

$$\begin{aligned}\mathcal{C}_{\mathcal{A}_3}(\widetilde{\mathcal{F}}) &= \mathbb{E}_{x \sim D_0} \mathbb{E}_{W_R \sim \mathcal{U}_{m,n}(\lambda)} [\mathbf{I}(\widehat{B}_{\mathcal{F}}(x + \rho \text{sign}(\frac{\nabla L(\widetilde{\mathcal{F}}(x), y)}{\nabla x})) \neq \widehat{B}_{\mathcal{F}}(x))] \\ &= \frac{1}{2^n} \mathbb{E}_{x \sim D_0} [\sum_{V \in \{-1, 1\}^n} P_{W_R \sim \mathcal{U}_{m,n}(\lambda)} (\text{sign}(\frac{\nabla L(\widetilde{\mathcal{F}}(x), y)}{\nabla x}) = V) Q(x, V, \rho)] \\ &\leq (T(\lambda, \mu)/2)^n \mathbb{E}_{x \sim D_0} [(\sum_{V \in \{-1, 1\}^n} Q(x, V, \rho))] \\ &\leq (2T(\lambda, \mu))^n \mathcal{C}(\mathcal{F}, \rho)\end{aligned}$$

where $T(\lambda, \mu) = 1 - \frac{(2\lambda - \mu)^2}{8\lambda^2}$. We have $(2T(\lambda, \mu))^n = (2 - \frac{4\lambda^2 + \mu^2 - 4\lambda\mu}{4\lambda^2})^n = (1 + \frac{4\lambda\mu - \mu^2}{4\lambda^2})^n \leq (1 + \frac{\mu}{\lambda})^n \leq e^{n\mu/\lambda}$. Hence, $\mathcal{C}_{\mathcal{A}_3}(\lambda) < e^{n\mu/\lambda} \mathcal{C}(\mathcal{F}, \rho)$. \square

5 Experiments

5.1 Accuracy of the bias classifier

In this section, we give the accuracy of the bias classifier using the MNIST and CIFAR-10 data sets. We compare two models, whose detailed structure can be found in the appendix.

$\mathcal{F}^{(1)}$: trained with adversarial trianing (5).

$\mathcal{F}^{(2)}$: trained with Algorithm 1.

Then, we use $B_{\mathcal{F}^{(2)}}(x)$ as the classifier. We test the accuracy on the test set (TS) and the strong adversaries (SA, see [36]) and the results are given in Table 2. From the table, we can see that the bias classifiers achieve higher accuracies than $\mathcal{F}^{(1)}$ in most cases and in particular for the more difficult strong adversaries.

Network	TS/MNIST	SA/MNIST	TS/CIFAT-10	SA/CIFAT-10
$\mathcal{F}^{(1)}$	99.19%	51.5%	81.23%	19%
$B_{\mathcal{F}^{(2)}}$	99.12%	87.5%	82.84%	42%

Table 2: Accuracies for MNIST and CIFAR-10

Moreover, for CIFAR-10, we compare the accuracy of our network and two other networks ResNet18 and VGG19, all using adversarial training. From the results in Table 3, our network $\mathcal{F}^{(1)}$ performs better than ResNet18 and VGG 19.

Network	Test Set	Strong adversaries
$\mathcal{F}^{(1)}$	81.23%	19%
ResNet18	80.64%	9%
VGG19	78.92%	12%

Table 3: Accuracies for three networks on CIFAR-10.

As pointed out in [38], networks trained with adversarial training are usually have lower accuracies, and the accuracies given in Tables 2 and 3 are about the best ones for DNN models of similar size.

5.2 Robustness of the bias classifier against original-model attack

In this section, we check the robustness of the bias classifier against the original-model attack given in Algorithm 2.

5.2.1 Experimental results

We use two more networks: $\mathcal{F}^{(3)}$ has the same structure with $\mathcal{F}^{(1)}$ given in Section 5.1, but trained with the first-order regulation method [25], and $\mathcal{F}^{(4)}$ has the same structure with $\mathcal{F}^{(1)}$, but trained with the adversarial training by trades [38]. Six kinds of adversaries are used:

l_∞ adversaries: 1- i ($i = 1, 2, 3$). Each pixel of the sample changes at most $0.i$. PGD [20] is used to attack: each step changes 0.01 and moves $10i$ steps.

l_0 adversaries: 2- i ($i = 40, 60, 80$). Change at most i pixels of the sample JSMA [21] is used to attack: change $20i + 20$ pixel and each of these pixels can change at most 1.

The results are given in Tables 4 and 5. The first four rows are the creation rates of adversaries for $\mathcal{F}^{(1)}, \mathcal{F}^{(2)}, \mathcal{F}^{(3)}, \mathcal{F}^{(4)}$ with method PGD [20] for l_∞ adversaries and JSMA [21] for l_0 adversaries. The last two rows are the generation rates of adversaries for the original-model attack of the bias classifiers.

Network	1-1	1-2	1-3	2-40	2-60	2-80
$\mathcal{F}^{(1)}$	3%	17%	55%	55%	79%	87%
$\mathcal{F}^{(2)}$	4%	22%	77%	62%	82%	90%
$\mathcal{F}^{(3)}$	22%	78%	99%	75%	98%	99%
$\mathcal{F}^{(4)}$	4%	15%	53%	62%	77%	88%
$B_{\mathcal{F}^{(1)}}$	2%	7%	13%	35%	43%	46%
$B_{\mathcal{F}^{(2)}}$	2%	2%	3%	39%	50%	53%

Table 4: Creation rates of adversaries for MNIST

Network	1-0.1	1-0.2	1-0.3	2-40	2-60	2-80
$\mathcal{F}^{(1)}$	54%	77%	90%	72%	85%	96%
$\mathcal{F}^{(2)}$	54%	72%	85%	69%	88%	97%
$\mathcal{F}^{(3)}$	88%	92%	99%	89%	99%	99%
$\mathcal{F}^{(4)}$	49%	73%	85%	70%	89%	97%
$B_{\mathcal{F}^{(1)}}$	67%	70%	86%	70%	84%	91%
$B_{\mathcal{F}^{(2)}}$	41%	58%	77%	49%	73%	84%

Table 5: Creation rates of adversaries for CIFAR-10

From the tables, we can see that the bias classifiers $B_{\mathcal{F}^{(2)}}$ has significant lower creation rates of adversaries than all other networks. For l_∞ adversaries of MNIST, $B_{\mathcal{F}^{(2)}}$ achieves near optimal results and the adversaries almost disappear. For CIFAR-10, the creation rates of adversaries are still quite high comparing to that of MNIST. We will explain the reason in Section 5.2.2.

5.2.2 Influence of adversarial training on the bias classifier

We use PGD [20] to create adversaries and show how $B_{\mathcal{F}_y}(x)$ and $\mathcal{F}_y(x)$ change along with the steps of the adversarial training to show the results in Tables 4 and 5.

In Figure 1, we give the data of using the network Lenet-5 [17] for a sample x_A with label y in MNIST. The blue, orange, green lines in the first picture are $\text{Softmax}\mathcal{F}_y(x)$, $\text{Softmax}B_{\mathcal{F}_y}(x)$, $\text{Softmax}W_{\mathcal{F}_y}(x)$, respectively. The blue, orange, green lines in the second picture are $\mathcal{F}_y(x)$, $B_{\mathcal{F}_y}(x)$, $W_{\mathcal{F}_y}(x)$, respectively.

When the blue line decreases, we obtain an adversary for \mathcal{F} , which is not an adversary of $B_{\mathcal{F}}$, because $\text{Softmax}B_{\mathcal{F}_y}(x)$ does not reduce significantly. For most samples from MNIST, the pictures are almost like this one, so the values of lines 4-5 in Table 4 are low.

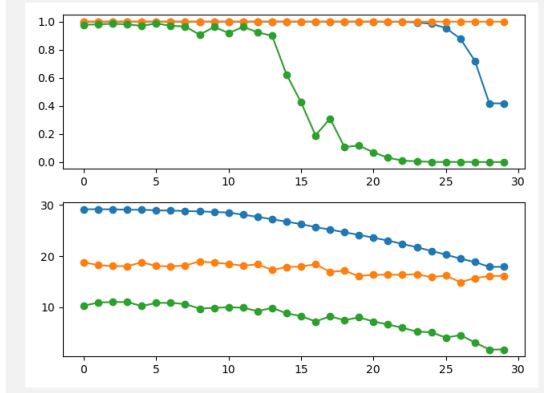


Figure 1: Values of $\mathcal{F}_y(x)$, $B_{\mathcal{F}_y}(x)$ and $W_{\mathcal{F}_y}(x)$ along with the adversarial training steps

Similar results are given in Figures 2 for CIFAR-10 and network VGG-19 [26]. In this case, the adversary of \mathcal{F} is also an adversary of $B_{\mathcal{F}}$. This explains why the values of lines 4-5 in Table 5 are higher than that of Table 4.

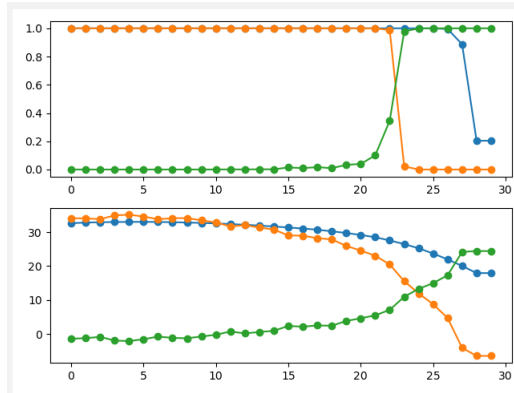


Figure 2: Values of $\mathcal{F}_y(x)$, $B_{\mathcal{F}_y}(x)$ and $W_{\mathcal{F}_y}(x)$ along with the adversarial training steps

5.3 Safety against the original-model gradient-based attack

In this section, we use experimental results to validate Theorems 4.1 and 4.3.

5.3.1 Existence rates of adversaries

In this section, we give the approximate rates of a random sample in a small neighbourhood of a sample in the training set to be an adversary. This information will be used to show the robustness of the bias classifier.

Three ways to select random samples are used for a given sample x in the test set (In there, x has been given the correct label by the network.).

R_1 : Randomly select 60 pixels of x and change each pixel from b to $1 - b$.

R_2 : Each pixel of x is added by a random number $0.2U(-1, 1)$, where $U(-1, 1)$ is the binomial distribution of 1 and -1 .

The network $B_{\mathcal{F}^{(2)}}$ in Section 5.1 is compared with two networks:

\mathcal{N}_1 : Lenet-5 for MNIST and VGG-19 for CIFAR-10, with normal training (2).

\mathcal{N}_2 : Lenet-5 for MNIST and VGG-19 for CIFAR-10, with adversarial training (5).

In Table 6, we give the average creation rates of adversaries. From the table, we can see that the random adversary creation rates are quite low for networks \mathcal{N}_2 and $B_{\mathcal{F}^{(2)}}$ trained with the adversarial training.

Network	R_1/MNIST	R_2/MNIST	$R_1/\text{CIFAR-10}$	$R_2/\text{CIFAR-10}$
\mathcal{N}_1	0.77%	1.47%	13.31%	11.81%
\mathcal{N}_2	1.00%	1.02%	4.69%	2.49%
$B_{\mathcal{F}^{(2)}}$	0.85%	1.64%	4.28%	1.67%

Table 6: Random adversary creation rates.

5.3.2 Safety of the bias classifier against original-model gradient-based attack

For MNIST, let $\mathcal{F}^{(5)} = \mathcal{F}^{(2)} + W_5x$, where $\mathcal{F}^{(2)}$ is given in Section 5.1 and $W_5 \in \mathbb{R}^{10 \times 784}$ is selected from $\mathcal{U}_{10,784}(\lambda)$ for $\lambda = 100$.

For CIFAR-10, let $\mathcal{F}^{(6)} = \mathcal{F}^{(2)} + W_6x$, where $\mathcal{F}^{(2)}$ is given in Section 5.1 and $W_6 \in \mathbb{R}^{10 \times 3072}$ is selected from $\mathcal{U}_{10,3072}(\lambda)$ for $\lambda = 100$.

The creation rates of adversaries of the original-model gradient-based attack are given in Table 7, where the adversaries are introduced in Section 5.2.1 and the data.

Network	1-1	1-2	1-3	2-40	2-60	2-80
$B_{\mathcal{F}^{(5)}}$ for MNIST	1%	2%	2%	2%	3%	4%
$B_{\mathcal{F}^{(6)}}$ for CIFAR-10	19%	20%	22%	21%	22%	24%

Table 7: Original-model gradient-based attack for MNIST and CIFAR-10

From the first row of Table 7, the bias classifier is safe against the original-model gradient-based attack for MNIST. For MNIST, the adversarial creation rates in Table 7 are near the adversarial rates of random samples in Table 6. Furthermore, the results are also better than that given in Table 4, especially for the l_∞ adversaries.

From the second row of Table 7, the results are also near optimal for CIFAR-10. First, comparing to the results of original-model attack in Table 5, the adversary creation rates are decreased by half.

Second, from Table 3, the accuracy of the bias classifier is about 82%. The adversary creation rates in Table 7 are about 20%-24%. Combining these two sets of data, the real adversary creation rates are about 1% – 6% which are just above the random creation rates of adversaries given in Table 6.

5.4 Black-box attack on the bias classifier

In this section, we use the transfer-based black-box attack [29] to compare three networks: $\mathcal{F}^{(1)}$, $\mathcal{F}^{(3)}$, $\mathcal{F}^{(4)}$, $B_{\mathcal{F}^{(2)}}$ defined in Sections 5.1 and 5.2.1.

The transfer-based black-box attack for a network \mathcal{F} works as follows. A new network $\bar{\mathcal{F}}$ is trained with the training set $\{(x, \mathcal{F}(x))\}$ for certain samples x . Then, we use PGD and JSMA to create adversaries for $\bar{\mathcal{F}}$ and check whether they are adversaries of \mathcal{F} . The results are given in Table 8. We can see that, the bias classifier performs better for most difficult adversaries and in particular for l_∞ adversaries. Also, the adversary creation rates are about half of that of the original-model attack in Tables 4 and 5. So the bias classifier has better robustness for black-box attack in most cases.

Model	1-1	1-2	1-3	2-40	2-60	2-80
$\mathcal{F}^{(1)}$	1%	2%	18%	28%	35%	40%
$\mathcal{F}^{(3)}$	6%	12%	28%	38%	45%	50%
$\mathcal{F}^{(4)}$	1%	3%	21%	24%	39%	46%
$B_{\mathcal{F}^{(2)}}$	3%	5%	13%	24%	30%	37%

Table 8: Creation rates of adversaries for black-box attack of MNIST

Model	1-0.1	1-0.2	1-0.3	2-40	2-60	2-80
$\mathcal{F}^{(1)}$	22%	23%	28%	35%	36%	41%
$\mathcal{F}^{(3)}$	27%	29%	36%	40%	43%	50%
$\mathcal{F}^{(4)}$	21%	24%	28%	33%	39%	44%
$B_{\mathcal{F}^{(2)}}$	21%	23%	24%	33%	36%	41%

Table 9: Creation rates of adversaries for black-box attack of CIFAR-10

5.5 Correlation attack

In this section, it is shown that the bias classifier is safe against the correlation attack proposed in section 3.3. The network used here is $\mathcal{F}^{(2)}$ given in Section 5.1 and the data set is CIFAR-10. In Table 10, we give the adversary creation rates for samples which are given the correct label by $B_{\mathcal{F}^{(2)}}$. Comparing to results in Tables 5 and 9, we can see that the bias classifier is quite safe against the correlation attack.

Network	1-0.1	1-0.2	1-0.3	2-40	2-60	2-80
$B_{\mathcal{F}^{(2)}}$	4%	11%	12%	8%	17%	21%

Table 10: Adversary creation rates for CIFAR-10 with the correlation attack

In Figure 3, we give the attack procedure. It can be seen that when $(W_{x,y} - W_{x,i})x$ increases $B_{x,y} - B_{x,i}$ indeed decrease, but $B_{x,y} - B_{x,i}$ does not decrease enough to change the label, where y is the label of x and $i \neq y$.

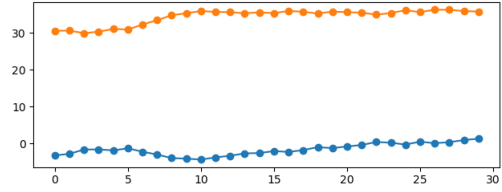


Figure 3: The x -axis is number of steps of the attack. The blue line is $(W_{x,9} - W_{x,0})x$ and the orange line $B_{x,9} - B_{x,0}$. We compare the values for images of 9 and 0.

5.6 Comparison with other methods to defend adversaries

In this section, we compare our model with several existing models. We use PGD-20 with l_∞ bound $\epsilon = 8/255$ to create adversaries on the test set of CIFAR-10.

In Table 11, we give the adversary creation rates under various attacks. The network structure of our model is $\mathcal{F}^{(2)}$ in section 5.1 and ResNet-10 [13] for other networks. The results for other networks are from the cited papers. Our model cannot use gradient directly, so we use the original-model attack given in Section 3.2.

Attack Method	Adversary creation rates
ADV [20]	57.1%
TRADE [38]	54.7%
MMA [30]	62.7%
FOAR [25]	67.7%
SOAR [19]	44.0%
$B_{\mathcal{F}^{(2)}}$ in Sec. 5.1	41.1%
$B_{\mathcal{F}^{(6)}}$ in Sec. 5.3.2	20%

Table 11: Adversary creation rates under various attacks for CIFAR-10

Although the structures of the networks are not the same and the way to attack is not the same, this comparison give a rough idea of the performance that can be achieved for various methods of defending adversaries. As we explained in Section 5.3.2, 20% is near the optimal results since the accuracy is about 82% for this dataset.

5.7 Summary of the experiments

We give a summary of the experiments in this section. From Table 6, we can see that the bias classifier with a random first-degree part is safe against adversaries.

From Tables 5, 9, 10, the original-model attack, the black-box attack, and the correlation attack become weaker for creating adversaries, and the original model attack is the best available attack for the bias classifier.

From Table 11, we see that the attack method SOAR [19] and the classifier achieve the best results for creating lower rates of adversaries, which is about the half of that the optimal rates achieved by $B_{\mathcal{F}_B^{(6)}}$.

6 Concluding remarks

In this paper, we show that the bias part of a DNN can be effectively trained as a classifier. The motivation to use the bias part as the classifier is that gradients of the DNN seems to be inevitable to generate adversaries efficiently and the bias part of a DNN with Relu as activation functions is a piecewise constant function with zero gradient and is safe against direct gradient-based attacks such as FGSM.

The bias classifier can be effectively trained with the adversarial training method [20], because this training method increases the classification power of the bias part and decreases the classification power of first-degree part when a new loss function is used. Experimental results are used to show the robustness of the bias classifier over the standard DNNs

Finally, adding a random first-degree part to the bias classifier, an information-theoretically safe classifier is obtained, that is, its adversary generate adversaries are almost the same as the rate of random samples to be adversaries.

References

- [1] N. Akhtar and A. Mian. Threat of Adversarial Attacks on Deep Learning in Computer Vision: A Survey. arXiv:1801.00553v3, 2018.
- [2] A. Athalye, N. Carlini, D. Wagner. Obfuscated Gradients Give a False Sense of Security: Circumventing Defenses to Adversarial Examples. *Proc. ICML'2018*, 274-283, 2018.
- [3] A. Azulay and Y. Weiss. Why Do Deep Convolutional Networks Generalize so Poorly to Small Image Transformations? *Journal of Machine Learning Research*, 20, 1-25, 2019.
- [4] T. Bai, J. Luo, J. Zhao. Recent Advances in Understanding Adversarial Robustness of Deep Neural Networks. arXiv:2011.01539, 2020.
- [5] M. Cisse, P. Bojanowski, E. Grave, Y. Dauphin, N. Usunier. Parseval Networks: Improving Robustness to Adversarial Examples. *Proc. ICML'2017*, 854-863, 2017.
- [6] J. Cohen, E. Rosenfeld, Z. Kolter. Certified adversarial robustness via randomized smoothing. *Proc. ICML'2019*, PMLR, 1310-1320, 2019.
- [7] G. Cybenko. Approximation by Superpositions of a Sigmoidal Function. *Mathematics of control, signals and systems*, 2(4), 303-314, 1989.
- [8] C. Etmann, S. Lunz, P. Maass, C.B. Schönlieb. On the Connection Between Adversarial Robustness and Saliency Map Interpretability. arXiv preprint arXiv:1905.04172, 2019.
- [9] O. Goldreich. *Foundations of Cryptography, Volume II, Basic Tools*. Cambridge University Press, 2009.
- [10] I.J. Goodfellow, Y. Bengio, A. Courville. *Deep Learning*, MIT Press, 2016.
- [11] I.J. Goodfellow, J. Shlens, C. Szegedy. Explaining and Harnessing Adversarial Examples. arXiv:1412.6572, 2014.
- [12] C. Guo, M. Rana, M. Cisse, L. van der Maaten. Countering Adversarial Images using Input Transformations. arXiv preprint arXiv:1711.00117, 2017.

- [13] K. He, X. Zhang, S. Ren, J. Sun. Deep Residual Learning for Image Recognition. *Proc. CVPR*, 770-778, 2016.
- [14] M. Hein and M. Andriushchenko. Formal Guarantees on the Robustness of a Classifier Against Adversarial Manipulation. *Proc. NIPS*, 2266-2276, 2017.
- [15] G. Hinton, O. Vinyals, J. Dean. Distilling the Knowledge in a Neural Network. arXiv:1503.02531, 2015.
- [16] M. Lecuyer, V. Atlidakis, R. Geambasu, D. Hsu, S. Jana. Certified Robustness to Adversarial Examples with Differential Privacy. *IEEE Symposium on Security and Privacy*, 656-672, 2019.
- [17] Y. LeCun, L. Bottou, Y. Bengio, P. Haffner. Gradient-based Learning Applied to Document Recognition. *Proc. of the IEEE*, 86(11), 2278-2324, 1998.
- [18] Y. LeCun, Y. Bengio, G. Hinton. Deep Learning, *Nature*, 521(7553), 436-444, 2015.
- [19] A. Ma, F. Faghri, N. Papernot, A.M. Farahmand. SOAR: Second-Order Adversarial Regularization. arXiv:2004.01832, 2020.
- [20] A. Madry, A. Makelov, L. Schmidt, D. Tsipras, A. Vladu. Towards Deep Learning Models Resistant to Adversarial Attacks. arXiv:1706.06083, 2017.
- [21] N. Papernot, P. McDaniel, S. Jha, M. Fredrikson, Z.B. Celik, A. Swami. The Limitations of Deep Learning in Adversarial Settings. *IEEE European symposium on security and privacy*, 372-387, 2016.
- [22] A. Sanyal, V. Kanade, P.H.S. Torr P.K. Dokania. Robustness via Deep Low-rank Representations. arXiv:1804.07090, 2018.
- [23] A. Shafahi, W.R. Huang, C. Studer, S. Feizi, T. Goldstein. Are Adversarial Examples Inevitable? arXiv:1809.02104, 2018.
- [24] A. Shafahi, M. Najibi, A. Ghiasi, Z. Xu, J. Dickerson, C. Studer, L.S. Davis, G. Taylor, T. Goldstein. Adversarial Training for Free! ArXiv: 1904.12843, 2019.
- [25] C.J. Simon-Gabriel, Y. Ollivier, L. Bottou L, D. Lopez-Paz. First-order Adversarial Vulnerability of Neural Networks and Input Dimension. *ICML*, 5809-5817, 2019.
- [26] K. Simonyan and A. Zisserman. Very Deep Convolutional Networks for Large-scale Image Recognition. arXiv preprint arXiv:1409.1556, 2014.
- [27] C. Szegedy, W. Zaremba, I. Sutskever, J. Bruna, D. Erhan, I.J. Goodfellow, R. Fergus. Intriguing Properties of Neural Networks. arXiv:1312.6199, 2013.
- [28] F. Tramer, A. Kurakin, N. Papernot, I. Goodfellow, D. Boneh, P. McDaniel. Ensemble Adversarial Training: Attacks and Defenses. ArXiv: 1705.07204, 2017.
- [29] F. Tramér, N. Papernot, I. Goodfellow, D. Boneh, P. McDaniel. The Space of Transferable Adversarial Examples. arXiv preprint arXiv:1704.03453, 2017.
- [30] Z. Wang, C. Xiang, W. Zou, C. Xu. MMA Regularization: Decorrelating Weights of Neural Networks by Maximizing the Minimal Angles. arXiv:2006.06527, 2020.

- [31] C. Xie, J. Wang, Z. Zhang, Z. Ren, A. Yuille. Mitigating Adversarial Effects Through Randomization. arXiv:1711.01991, 2017.
- [32] C. Xie, Y. Wu, L.V.D. Maaten, A.L. Yuille, K. He. Feature Denoising for Improving Adversarial Robustness. CVPR, 501-509, 2019.
- [33] H. Xu, Y. Ma, H.C. Liu, D. Deb, H. Liu J.L. Tang, A.K. Jain. Adversarial Attacks and Defenses in Images, Graphs and Text: A Review. *International Journal of Automation and Computing*, 17(2), 151-178, 2020.
- [34] M. Wen, Y. Xu, Y. Zheng, Z. Yang, X. Wang. Sparse Deep Neural Networks Using $L_{1,\infty}$ -Weight Normalization, *Statistica Sinica*, 31, 1397-1414, 2021
- [35] L. Yu and X.S. Gao. Improve the Robustness and Accuracy of Deep Neural Network with $L_{2,\infty}$ Normalization. arXiv:2010.04912.
- [36] L. Yu and X.S. Gao. A Robust Classification-autoencoder to Defend Outliers and Adversaries. arXiv preprint arXiv:2106.15927, 2021.
- [37] X.Y. Zhang, C.L. Liu, C.Y. Suen. Towards Robust Pattern Recognition: A Review. *Proc. of the IEEE*, 108(6), 894-922, 2020.
- [38] H. Zhang, Y. Yu, J. Jiao, E.P. Xing, L.E. Ghaoui, M.I. Jordan. Theoretically Principled Trade-off between Robustness and Accuracy. *Proc. ICML*, 2019.
- [39] Moosavi-Dezfooli S M, Fawzi A, Frossard P. Deepfool: a simple and accurate method to fool deep neural networks[C]//Proceedings of the IEEE conference on computer vision and pattern recognition. 2016: 2574-2582.

Appendix. Structures of DNN models used in the experiments

The network in section 5.1:

Networks $\mathcal{F}^{(1)}$ and $\mathcal{F}^{(2)}$ for MNIST have the same structure:

Input layer: $N \times 1 \times 28 \times 28$, where N is steps of training.

Hidden layer 1: a convolution layer with kernel $1 \times 32 \times 3 \times 3$ with padding= 1 → do a batch normalization → do Relu → use max pooling with step=2.

Hidden layer 2: a convolution layer with kernel $32 \times 64 \times 3 \times 3$ with padding= 1 → do a batch normalization → do Relu → use max pooling with step=2.

Hidden layer 3: a convolution layer with kernel $64 \times 128 \times 3 \times 3$ with padding= 1 → do a batch normalization → do Relu → use max pooling with step=2.

Hidden layer 4: draw the output as $N \times 128 \times 3 \times 3$ → use a full connection with output size $N \times 128 \times 2$ → do Relu.

Hidden layer 4: use a full connection with output size $N \times 100$ → do Relu.

Output layer: a full connection layer with output size $N \times 10$.

Networks $\mathcal{F}^{(1)}$ and $\mathcal{F}^{(2)}$ for CIFAR-10 have the same structure:

Input layer: $N \times 3 \times 32 \times 32$, where N is steps of training.

Hidden layer 1: a convolution layer with kernel $3 \times 64 \times 3 \times 3$ with padding= 1 → do a batch normalization → do Relu.

Hidden layer 2: a convolution layer with kernel $64 \times 64 \times 3 \times 3$ with padding= 1 → do a batch normalization → do Relu.

Hidden layer 3: a convolution layer with kernel $64 \times 128 \times 3 \times 3$ with padding= 1 → do a batch normalization → do Relu.

Hidden layer 4: a convolution layer with kernel $128 \times 128 \times 3 \times 3$ with padding= 1 → do a batch normalization → do Relu → use max pooling with step=2.

Hidden layer 5: a convolution layer with kernel $128 \times 256 \times 3 \times 3$ with padding= 1 → do a batch normalization → do Relu.

Hidden layer 6: a convolution layer with kernel $256 \times 256 \times 3 \times 3$ with padding= 1 → do a batch normalization → do Relu.

Hidden layer 7: a convolution layer with kernel $256 \times 256 \times 3 \times 3$ with padding= 1 → do a batch normalization → do Relu → use max pooling with step=2.

Hidden layer 8: a convolution layer with kernel $256 \times 512 \times 3 \times 3$ with padding= 1 → do a batch normalization → do Relu.

Hidden layer 9: a convolution layer with kernel $512 \times 512 \times 3 \times 3$ with padding= 1 → do a batch normalization → do Relu.

Hidden layer 10: a convolution layer with kernel $512 \times 512 \times 3 \times 3$ with padding= 1 → do a batch normalization → do Relu → use max pooling with step=2.

Hidden layer 11: a convolution layer with kernel $512 \times 512 \times 3 \times 3$ with padding= 1 → do a batch normalization → do Relu.

Hidden layer 12: a convolution layer with kernel $512 \times 512 \times 3 \times 3$ with padding= 1 → do a batch normalization → do Relu.

Hidden layer 13: a convolution layer with kernel $512 \times 512 \times 3 \times 3$ with padding= 1 → do a batch normalization → do Relu → use max pooling with step=2.

Hidden layer 14: draw the output as $N \times 2048$ → a full connection layer with output size $N \times 1024$ → do Relu.

Hidden layer 15: a full connection layer with output size $N \times 512$ → do Relu.

Hidden layer 16: a full connection layer with output size $N \times 128$ → do Relu.

Output layer: a full connection layer with output size $N \times 10$.